$S = 1$ and $S = 2$ wave functions. The spectrum in Figure 5 is approaching this limit. The simulated spectrum does not adequately account for the differences in the line widths of the transitions in this limit but does indicate the positions of the turning points in the spectrum. The calculated spectrum was obtained with $J = 0.27$ cm^{-1}, $r = 6$ Å, $\epsilon = 35°$, and $\eta = 75°$. The values of r and ϵ are consistent with CPK molecular models of the complex.

Trends in the Values of J. The values of J (Table I) were consistently larger for the same substituent at the 4-position of the pyridine ring than at the 3-position, as expected for predominantly π delocalization of the metal unpaired spin density into the pyridine ring. The interaction was weaker through amide linkages than through the Schiff base linkage, which is also consistent with predominantly π delocalization. The stronger interaction for the urea linkage (XI) than for the analogous amide (VI) was observed previously for vanadyl complexes with predominantly π delocalization but not for copper(II) complexes with predominantly σ delocalization.[13] Thus the trends in the values of J are consistent with π delocalization due to interaction of the partially filled chromium d_{xz}, d_{yz} orbitals with the pyridine π system.

Comparison with VO(tfac)$_2$·L. Table I summarizes the values of J that have been obtained for VO(tfac)$_2$·L and Cr(TPP)Cl·L. The vanadyl complexes were studied in fluid solution[12,13] and (for some of the ligands) on imbiber beads at −180 °C.[14] The values of J did not appear to be strongly temperature dependent. It therefore seems reasonable to compare these values for the vanadyl complexes with the values of J obtained for the Cr(TPP)Cl complexes obtained at −180 °C. The ligands in Table I are arranged in the order of increasing values of J for the VO(tfac)$_2$ complexes. The values of J for the chromium complexes follow the same patterns as the vanadyl complexes. Thus it is evident that the trends in the values of J observed for one metal with primarily π delocalization into a spin-labeled pyridine are transferrable to another metal with primarily π delocalization. We had previously observed that trends in the values of J observed for spin-labeled pyridines bound to two $S = {}^1/_2$ metals (Cu(II) and low spin Co(II)) with predominantly σ delocalization were similar.[19] Thus it appears that if two metals have similar mechanisms of spin delocalization into the orbitals of the spin-labeled ligand, the trends in the values of J are similar.

The values of J for the chromium complexes were about $^1/_2$ to $^2/_3$ of the values observed for the vanadyl complexes. If the number of unpaired electrons on the metal were the only difference between the two sets of complexes, a factor of $^1/_3$ would be expected.[6] The lower oxidation state of the chromium in Cr(TPP)Cl than of vanadium in VO(tfac)$_2$ may cause a greater spin delocalization of the chromium unpaired electrons than of the vanadyl unpaired electron. Although the geometry of the metalloporphyrin complex is fairly rigidly defined, the geometry of the vanadyl complex may be distorted, thereby decreasing the effectiveness of the overlap between the metal and pyridine orbitals.

Acknowledgment. The partial support of this work by NIH Grant GM 21156 is gratefully acknowledged. Purchase of the IBM ER200 EPR spectrometer was funded in part by NSF Grant CHE8411282. Purchase of the Harris H1000 computer was funded in part by a grant from the Harris Corp. We thank Prof. Belford for a copy of his fourth-order frequency shift perturbation routine and for useful discussions concerning its use.

Registry No. Cr(TPP)Cl·I, 104090-04-2; Cr(TPP)Cl·II, 104090-05-3; Cr(TPP)Cl·III, 104090-06-4; Cr(TPP)Cl·IV, 104172-20-5; Cr(TPP)Cl·V, 104090-07-5; Cr(TPP)Cl·VI, 104172-21-6; Cr(TPP)Cl·VII, 104113-69-1; Cr(TPP)Cl·VIII, 104090-08-6; Cr(TPP)Cl·IX, 104090-09-7; Cr(TPP)Cl·X, 104090-10-0; Cr(TPP)Cl·XI, 104090-11-1; Cr(TPP)Cl·XII, 104090-12-2; Cr(TPP)Cl·XIII, 104090-13-3.

(19) Eaton, S. S.; Boymel, P. M.; Sawant, B. M.; More, J. K.; Eaton, G. R. *J. Magn. Reson.* **1984**, *56*, 183.

Contribution from the Department of Chemistry, University of Pittsburgh, Pittsburgh, Pennsylvania 15260

Electron Spin Resonance Studies of Copper(II) Polyamine and Imidazole Complexes

Shirin Siddiqui and Rex E. Shepherd*

Received August 20, 1985

ESR spectra were obtained in 50:50 Me_2SO/water glasses for CuL_4^{2+} and CuL_5^{2+} species (L = imH, $imCH_3$, py), for saturated polyamine donors (L = en, trien, tren, cyclam, tet a and tet b), and for mixed-ligand complexes including $Cu(en)L_2^{2+}$, $Cu(en)L_3^{2+}$, $Cu(dien)L^{2+}$, $Cu(dien)L_2^{2+}$, $Cu(trien)L^{2+}$, $Cu(trien)L_2^{2+}$, and $Cu(cyclam)L^{2+}$ and $Cu(tren)L^{2+}$ (L = imH, $imCH_3$, or py). The presence of at least one aromatic L donor either in-plane of a CuN_4 donor set (for example $Cu(dien)(imH)^{2+}$) or in the axial position of a CuN_5 donor set ($Cu(cyclam)(imH)^{2+}$) causes all N donors to contribute essentially equally to N-shf patterns in the $g_\perp$ region of the rhombically distorted axial ESR spectrum of the complex. Saturated polyamine complexes exhibit only very weak N-shf coupling in the absence of imidazoles or pyridine. ESR parameters for 36 Cu(II) imidazole, polyamine, or mixed-ligand complexes are reported in the Me_2SO/water glasses at 113 K. An approximate additivity of the influence of saturated N donors and aromatic N* donors in various $Cu(N,N^*)_4^{2+}$ and $Cu(N,N^*)_5^{2+}$ donor sets is observed.

Introduction

Cu(II) has been termed a "plastic" metal center[1a] due to the ability of a d^9 configuration to take on various modifications of coordination numbers 4, 5, and 6: square planar, tetragonal-distorted, rhombically distorted tetragonal, trigonal bipyramidal, and distorted octahedral.[2] Although it is convenient to describe complexes such as CuL_4^{2+} (L = NH_3, imH, py, $imCH_3$, etc.), $Cu(en)_2^{2+}$, $Cu(trien)^{2+}$, and $Cu(dien)L^{2+}$ as all CuN_4 species of approximately square-planar geometry, it is known from the sensitivity of ESR spectra that these species are not really equivalent in solution. A question of potential biochemical importance is whether or not one can determine the number of aromatic (imidazole or pyridine type) donor ligands in the presence of saturated N-bases (lysines, amines, etc.) that are present at a Cu(II) site from the ESR spectrum of a copper metalloprotein.

(1) (a) Gazo, J.; Bersuker, I. B.; Garaj, J.; Kabesova, M.; Kohout, J.; Langfelderova, H.; Melnik, M.; Serator, M.; Valach, F. *Coord. Chem. Rev.* **1976**, *19*, 253. (b) Margerum, D. W.; Cayley, G. R.; Weatherburn, D. C.; Pagenkopf, G. K. *Coordination Chemistry 2*; ACS Monograph 174; American Chemical Society: Washington, DC, 1978; p 1. (c) Wilkins, R. G. *The Study of Kinetics and Mechanism of Reactions of Transition Metal Complexes*; Allyn and Bacon: Boston, 1974; pp 200–201. (d) Basolo, F.; Pearson, R. G. *Mechanisms of Inorganic Reactions*, 2nd ed.; Wiley: New York, 1967; p 220.

(2) Hathway, B. J.; Billing, D. E. *Coord. Chem. Rev.* **1970**, *5*, 143.

0020-1669/86/1325-3869$01.50/0

Table I. ESR Parameters of CuL_n^{2+} Complexes (L = Aromatic or N* Donor) in Me_2SO/H_2O Glasses[a]

species	pH	$g_\parallel$	$g_\perp$	$10^4A_\parallel$(Cu), cm^{-1}	$A_\perp$(N), G	n
$Cu(imH)_4^{2+}$		2.31	2.06	154	14.9	4
$Cu(imCH_3)_4^{2+}$	6.6	2.29	2.06	171	15.0	4
$Cu(py)_4^{2+}$	6.3	2.30	2.06	167	15.0	4
		2.22[e]	...	174	14.0	4
$Cu(imH)_5^{2+}$	...	2.25	2.04 R	193	15.0	5
$Cu(imCH_3)_5^{2+}$	6.6	2.25	2.04 R	191	15.0	5
$^{63}Cu(imCH_3)_5^{2+}$	6.7	2.25	2.03 R	182	15.0	5
$Cu(imH)_6^{2+}$	7.65	2.24	2.04	181	14.9	4
$Cu(py)_5^{2+}$	6.6	2.27	2.05 R	190	15.0	5
$Cu(bpy)(H_2O)_2^{2+}$	...	2.29	2.06	169	15.0	2
$Cu(bpy)_2^{2+}$		2.27	2.06	164	14.5 W	2
$Cu(biimH)_2^{2+}$	3.6	2.25[b]	2.05	183	12	3
		2.25[c]	2.05	173	15	3 or 4
		2.25[d]	2.05	170	14.9	4
		2.26	2.06		...	...

[a] Legend: n = number of N ligand donors exhibiting N-shf; T = 113 K; pH 6–7; R = modest rhombic distortion; W = weak N-shf; imH = imidazole; $imCH_3$ = *N*-methylimidazole; biimH = 2,2′-biimidazole; bpy = 2,2′-bipyridine; py = pyridine. [b] CH_3NO_2/CH_3OH 9:1 glass. [c] CH_3NO_2/CH_3CN 9:1 glass. [d] Me_2SO/H_2O glass. [e] Reference 34.

EXAFS studies of $Cu(imH)_4^{2+}$ complexes show these systems are good models of plasma amine oxidase and related Cu(II) metalloproteins.[3]

A summary of some of the crucial features that have been observed in the studies of Cu(II)–(N-base) complexes is in order to simplify further discussion. Many of these statements have been confirmed in greater detail by the studies to be described in this paper. These include the general appearance of a frozen-solution or random-orientation spectrum and the presence or absence of N-superhyperfine coupling (N-shf) from the nitrogen ligand donors coordinated on Cu(II). An axial or C_{4v} environment about Cu(II) produces a four-line $g_\parallel$ region and a strong $g_\perp$ region in the first-derivative spectral presentation.[2,4] The fourth line derived from the $M_I = -^3/_2$ state may be overlapped with the more intense perpendicular line (containing all four transitions in the $g_\perp$ region as one unresolved line). A rhombic distortion produces a splitting of the $g_\perp$ region into a less intense g_{xx} line on the $g_\parallel$ side (low field) and a more intense $g_\perp$ (g_{yy}) line at higher field. N-shf coupling may appear on any of the lines, but it is generally more intense in the $g_\perp$ region, particularly on the low-field side of the axial spectrum or the lower field $g_\perp$ (g_{xx}) line of a rhombically distorted species. Empirically it has been observed that saturated N donors such as en in $Cu(en)_2^{2+}$ produce no, or at best very weak, N-shf lines.[4,8] Aromatized N* donors produce much stronger N-shf coupling patterns. Distortion of a Cu(II) complex away from D_{4h} or C_{4v} toward trigonal symmetry (D_{3h}) causes a substantial loss in N-shf coupling of all N or N* donors.[6] For example, in a 50:50 Me_2SO/H_2O glass $Cu(bpy)(H_2O)_4^{2+}$ shows a slightly rhombically distorted spectrum with five N-shf lines (from two N* donors; $g_\parallel$ = 2.29, $g_\perp$ = 2.06, $A_\parallel$ = 169[7]) whereas $Cu(bpy)_2^{2+}$, with four potential N* donors, shows only the weakest couplings (ca. five inflections on the $g_\perp$ line ($g_\parallel$ = 2.27, $g_\perp$ = 2.06, $A_\parallel$ = 164)). It is known from X-ray studies on $Cu(bpy)_2X^+$ (X = SCN^-, CN^-) that these complexes are trigonal ($\sim D_{3h}$)[2] and exhibit so-called reversed ESR spectra with $g_\perp$ at lower field. The trigonal distorted complexes also fail to exhibit N-shf coupling patterns. Addison[6] and Reed[9] have also shown that N*SN* ligands of the benzimidazole–thioether type tend to form distorted-square-pyramidal or T-shaped Cu(II) complexes with weak N-shf while Cu(II) complexes of tris(benzimidazolylmethyl)amine form trigonal-bipyramidal complexes[10] like the $[Cu(Me_6tren)X]^+$ complexes.[11] The trigonal-bipyramidal complexes do not show N-shf. The bis complexes of the bis(benzimidazole–thioether) type exhibit nine N-shf lines equal to four N* tetragonal donors.[6] With this background, we were interested to see whether N and N* donors could be differentiated within the same Cu(II) complex and what trends the overall geometries exhibit with changing degrees of chelation at Cu(II) with en, dien, trien, and tren. The details of the spectra and the best self-consistent interpretation of the results are described below.

Experimental Section

Cu(II) Salts. $[Cu(en)_2](NO_3)_2$, $[Cu(trien)](PF_6)_2$, $[Cu(dien)(H_2O)](NO_3)_2$, $[Cu(tren)(H_2O)](NO_3)_2$, and $[Cu(tren)(H_2O)](PF_6)_2$ were prepared by evaporation of a $Cu(NO_3)_2$ or $Cu(PF_6)_2$ solution of the appropriate polyamine. Ligands for $[Cu(tet\,a)(H_2O)](ClO_4)_2$ and $[Cu(tet\,b)(H_2O)](ClO_4)_2$ were prepared by the methods of Hay and Curtis.[5] $[Cu(biimH)_2](ClO_4)_2$ and the free ligand were prepared as described by Sakaguchi and Addison.[8] $Cu(acac)_2$ was prepared by precipitation from aqueous 2,4-pentanedione/$CuSO_4$ solution with pH adjustment. The product was recrystallized from hot solvents.

ESR Spectra. Spectra were recorded at 113 K with a Varian E-4 EPR spectrometer at 20 mW and 1.25-G modulation amplitude, tuned in the 9.07-GHz region. Cooling was provided by N_2 gas bubbled through liquid N_2. Solutions of the desired Cu(II) polyamine or Cu(II) amine complex at ca. 8.85×10^{-3} M were prepared at room temperature in 50% Me_2SO and 50% H_2O. Solutions were prepared from standard $Cu(NO_3)_2$ solution together with the desired ligand, usually with ~5% excess ligand to assure complexation. Various stoichiometries of a second ligand for the concentration-dependent studies were added as a known ratio to the Cu(II) complex in water and adjusted to the desired pH by addition of $HClO_4$ or NaOH solution. pH was measured with an Orion 701 meter using a glass/calomel assembly and standard commercial buffers (Fisher). Spectra of the solution species were also followed in the visible region with a Varian-Cary 118C spectrophotometer to examine for evidence of ligand addition, polyamine displacement, and major changes in ligand field or symmetry of the complex. Solutions were then mixed with an equal volume of Me_2SO and filled into narrow quartz EPR tubes for freezing at liquid-N_2 temperature. The frozen samples were placed under a flowing N_2 stream to establish control of the temperature with the Varian temperature-controller unit of the E-4 EPR instrument.

Organic Reagents. The following ligands were obtained from Aldrich: py, imH, $imCH_3$, bpy, Me_2en, Me_4en, en, dien, trien, histamine, 2-(2-aminoethyl)-1,3-propanediamine, 2-(aminomethyl)pyridine. Imidazole was recrystallized from benzene. All others were used as supplied. Abbreviations of ligands are given in Tables I and II. Solvents for the ESR glasses were dried over molecular sieves before use. The sources were as follows: Me_2SO, Baker; CH_3NO_2, Fisher; CH_3CN, Mallinck-

(3) (a) Scott, R. A.; Dooley, D. M. *J. Am. Chem. Soc.* **1985**, *107*, 4348. (b) Co, M. S.; Scott, R. A.; Hodgson, K. O. *J. Am. Chem. Soc.* **1981**, *103*, 986. (c) Suzuki, S.; Nakahara, T.; Oda, O.; Manabe, T.; Okuyama, T. *FEBS Lett.* **1980**, *116*, 17. (d) Yamada, H.; Yasunobu, K.; Yamano, T.; Mason, H. S. *Nature (London)* **1963**, *198*, 1092. (e) Hamilton, G. A. In *Copper Proteins*; Spiro, T. G., Ed.; Wiley: New York, 1981; pp 193–218.
(4) Bakalbassis, E.; Mrozinski, J.; Tsipis, C. A. *Inorg. Chem.* **1985**, *24*, 3548.
(5) Hay, R. W.; Lawrance, G. A.; Curtis, N. F. *J. Chem. Soc., Perkin Trans.* **1975**, *1*, 591.
(6) Addison, A. W.; Burke, P. J.; Hennick, K.; Nageswara, R.; Sinn, E. *Inorg. Chem.* **1983**, *22*, 3645.
(7) Entries in the text will be entered as $10^4A_\parallel$ in cm^{-1} unless the exponent is useful for clarity; i.e., 169×10^{-4} cm^{-1} will be written as 169 as is the frequent convention.
(8) Sakaguchi, U.; Addison, A. W. *J. Chem. Soc., Dalton Trans.* **1979**, 600.
(9) Dagdigian, J. V.; McKee, V.; Reed, C. A. *Inorg. Chem.* **1982**, *21*, 1332.
(10) Addison, A. W.; Hendricks, H. M.; Reedijk, J.; Thompson, L. K. *Inorg. Chem.* **1981**, *20*, 103.
(11) Barbucci, R.; Bencini, A.; Gatteschi, D. *Inorg. Chem.* **1977**, *16*, 2117.

Table II. ESR Parameters of Saturated Polyamine Cu(II) Complexes in Me_2SO/H_2O Glasses[a]

species	pH	$g_\parallel$	$g_\perp$	$10^4A_\parallel$, cm^{-1}	$A_\perp$(N), G	n
$Cu(en)(H_2O)_2^{2+}$		2.28	2.07 SR	178	12	1
		2.28[d]	2.06	181	...	...
$Cu(Me_4en)(H_2O)_2^{2+}$		2.28	2.06	168	13	1
$Cu(Me_2en)(H_2O)_2^{2+}$		2.28	2.07	172	12	1
$Cu(aepdn)(H_2O)^{2+}$		2.23	2.04	183	...	0
$Cu(tmdt)(NO_3)^+$		2.21[d]	...	178	...	...
$Cu(en)_2^{2+}$	5.4	2.20	2.05 SR	204	...	*b*
		2.21	2.05	203	11	...
$Cu(en)_2(NH_3)^{2+}$		2.21	2.05 SR	198	12	1
$Cu(trien)^{2+}$		2.20	2.07 SR	195	...	0
$Cu(cyclam)^{2+}$	5.4	2.18	2.09	221	14.9 VW	1
$Cu(tet\ a)^{2+}$ (red)		2.18	2.03	207	14.5 VW	4
		2.19[e]	2.05	206		
$Cu(tet\ a)^{2+}$ (blue)		2.19	2.04	163	...	0
$Cu(tet\ b)^{2+}$ (red)		2.40	2.07	123	16 VW	1
$Cu(tet\ b)^{2+}$ (blue)			2.14		98[c]	
$Cu(tren)(H_2O)^{2+}$		2.18			123[c]	

[a] Legend: SR = strong rhombic distortion; VW = very weak, but observable; en = ethylenediamine; Me_4en = 1,1′,4,4′-tetramethylethylenediamine; Me_2en = 1,1′-dimethylethylenediamine; tmdt = tetramethyldiethylenetriamine (Me_4dien); trien = triethylenetetramine; tren = tris(2-aminoethyl)-amine; aepdn = 2-(2-aminoethyl)-1,3-propanediamine. [b] Very weak features of g_{xx} region of $g_\perp$; n = 1 or 2. [c] $A_\perp$(Cu). [d] Reference 38. [e] Reference 42.

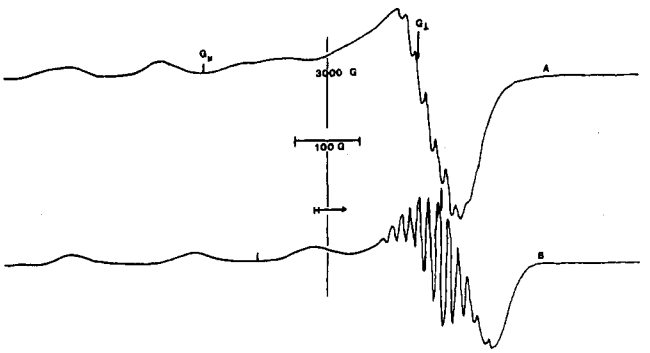

Figure 1. ESR spectra of Cu(II) imidazole complexes in Me_2SO/water glasses at 113 K: (A) $Cu(imH)_4^{2+}$, x = 4.0, 9.070 GHz; (B) $Cu(imH)_5^{2+}$, x = 10.0, 9.073 GHz.

rodt. The ligand cyclam was obtained from Strem Chemicals. Tren was obtained from Tridom Chemicals.

^{63}Cu Isotopic Studies. ^{63}Cu was obtained from Stholer Chemicals. The Cu foil was dissolved in concentrated nitric acid. The acidic $^{63}Cu(NO_3)_2$ solution was partially neutralized with NaOH. The labeled $^{63}Cu(NO_3)_2$ solution was used to prepare identical complexes of various ligand ratios in 50:50 H_2O/Me_2SO solvent as described above. Isotopic labeled $^{63}Cu(NO_3)_2$ and the $^{63,65}Cu(NO_3)_2$ naturally abundant mixture were reprepared from the HNO_3 reaction with pure metal foils of the ^{63}Cu isotope of a second lot and normal Cu foil. Identical results have been observed from all preparations.

Results and Discussion

Aromatic N*-Base Complexes. Spectra of $Cu(imH)_4^{2+}$ and $Cu(imH)_5^{2+}$ and related $imCH_3$ and py complexes were obtained in 50:50 Me_2SO/water glasses at 113 K. These are shown in Figure 1 for L = imH. Related spectra for L = $imCH_3$ and py appear in Figures 1sm–4sm (supplementary material). There is a distinct enhancement of the N-shf for n = 5 compared to that in n = 4 for the $Cu(imH)_n^{2+}$ spectra. The $Cu(imH)_5^{2+}$ spectrum remains constant for a [imH]:[Cu^{2+}] ratio of 5.0–10.0. Eleven N-shf lines are displayed for five N* donors with a modest tendency toward rhombic splitting of the $g_\perp$ line. Nine N-shf lines and even less rhombic distortion are seen for $Cu(imH)_4^{2+}$ (n = 4). The ESR spectrum of the CuL_5^{2+} complex is indicative of a slightly distorted square pyramid. When potential binding sites are to be filled by solvent, it will be assumed that H_2O fills the site for discussion purposes. There is no certainty that only H_2O, only Me_2SO, or a competition of these two solvents might actually describe the true situation in the Me_2SO/water glass. Virtually identical spectra were obtained at 50:50, 60:40, and 70:30 H_2O/Me_2SO solvent compositions for the $Cu(imH)_5^{2+}$ species. For simplicity the axial donors, if these are solvent, will be omitted from formulas in the text. The changing ligand field strength was also monitored by UV/visible spectroscopy of the ligand field bands. These spectra for $Cu(imH)_n^{2+}$ at x = 0, 1, 4, 5, 10, and 50 [imH]:[Cu^{2+}] ratios show the shifting maxima from 810 nm (x = 0), 760 nm (x = 1), 661 nm (x = 4), 640 nm (x = 5), 606 nm (x = 10), and 606 nm (x = 50). The UV/visible data imply that the ESR spectra shown in the frozen glass represent a composite of CuL_4^{2+} and CuL_5^{2+} at x = 5.0 and of CuL_4^{2+} and CuL_3^{2+} at x = 4.0. The overlap of the N-shf lines will reveal the species of higher coordination number when it is the dominant form in solution as A_N values are very similar for any of the three-, four-, five-, or six-coordinated species. The constancy of the UV/visible and ESR spectra in the range of x = 10.0–50.0 assures the correctness of the g values and A_{iso} parameters for the $Cu(imH)_5^{2+}$ species. Furthermore, at x = 200 the spectrum alters to give a species indicative of only four N* in-plane donors while the ligand field transition decreases slightly in energy (632 nm). The $g_\perp$ value shifts to a higher value at x = 200 compared to that at x = 50.0. These changes are only compatible if the ligand field strength of the five-coordinate species is higher than that of Jahn–Teller (J-T) distorted octahedral species; this result is correct on the basis of known splittings of d orbitals in these symmetries with NH_3 or N* field strength donors.[12] The J-T distorted "octahedral" complex, CuL_6^{2+}, is produced at x = 200. In this case the ligand field is actually relaxed with four in-plane strong Cu–N bonds and two weak axial N donors compared to the five strong interactions with the CuL_5^{2+} species where the "in-plane" donors can bend down in the C_{4v} complexes. Successive shifts in the $g_\perp$ region occur toward lower g_{xx} values with each additional N* donor for n = 1–5, followed by a final increase in g_{xx} for n = 6 (x = 200). This would not be the case if the species at x = 200 were only CuL_4^{2+}; furthermore, the number of N-shf lines would remain unexplained for the species giving 11 N-shf lines.

ESR parameters for various CuL_5^{2+} and CuL_4^{2+} species with L = imH, $imCH_3$, py, or bidentate equivalent ligands, biimH and bpy, are given in Table I. Figures in the text will be denoted as Figure 1A etc. while those in the supplementary material will be denoted as Figure 1sm etc. The value of $g_\parallel$ is smaller and $A_\parallel$ larger for n = 5 complexes vs. the values for n = 4. An inverse relationship in the magnitude of $g_\parallel$ and $A_\parallel$ is known for N_4, O_4, and S_4 donor sets for Cu(II).[6]

Literature reports list ESR parameters for $Cu(py)_4^{2+}$, $g_\parallel$ = 2.22, $A_\parallel$(Cu) = 174 G, and $A_\perp$(N) = 14 G,[13] and for $[Cu(imH)_4]$-

(12) (a) Douglas, B. E.; McDaniel, D. H.; Alexander, J. J. *Concepts and Models of Inorganic Chemistry*, 2nd ed.; Wiley: New York, 1983; Chapter 7. (b) Huheey, J. E. *Inorganic Chemistry: Principles of Structure and Reactivity*; Harper and Row: New York, 1978; Chapter 9.

(13) Wuthrich, K. *Helv. Chim. Acta* **1966**, *49*, 1400.

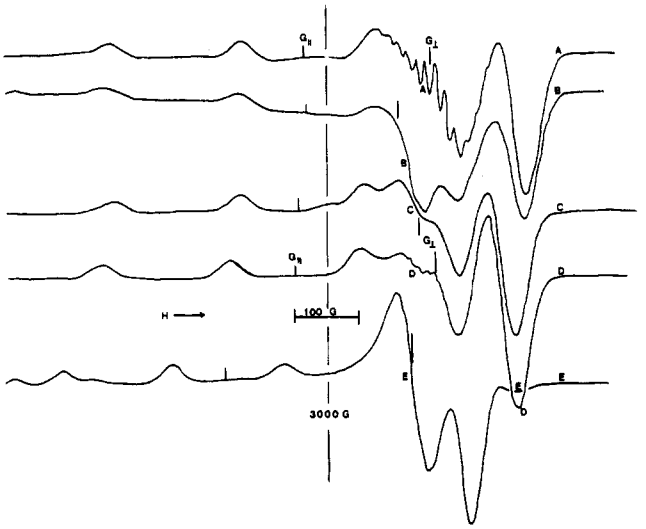

Figure 2. ESR spectra of Cu(II) polyamine complexes in Me_2SO/water glasses at 113 K: (A) Cu(cyclam)(imH)$^{2+}$, x = 1.0, 9.072 GHz, pH 7.80; (B) Cu(cyclam)$^{2+}$, 9.070 GHz, pH 5.40; (C) Cu(trien)$^{2+}$, 9.071 GHz, pH 5.30; (D) Cu(en)$_2^{2+}$, x = 2.0, 9.073 GHz, pH 6.54; (E) Cu(en)$(H_2O)_2^{2+}$, x = 1.0, 9.071 GHz, pH 5.85.

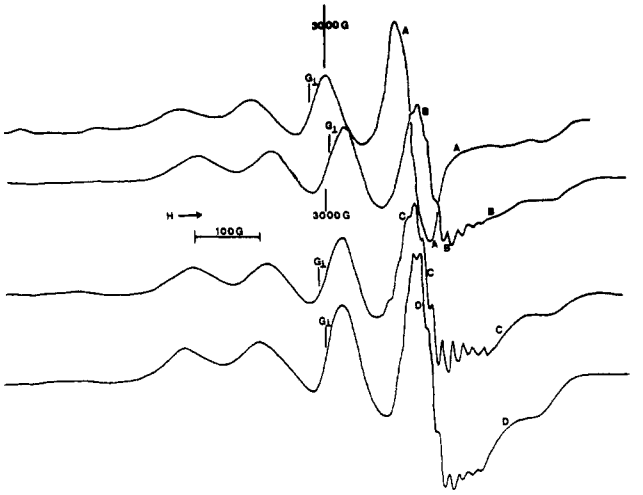

Figure 3. ESR spectra of Cu(tren)L^{2+} complexes in Me_2SO/water glasses at 113 K: (A) L = H_2O, 9.073 GHz, pH 5.52; (B) L = imH, x = 50.0, 9.072 GHz, pH 6.67; (C) L = $imCH_3$, x = 6.0, 9.073 GHz, pH 6.62; (D) L = py, x = 10.0, 9.073 GHz, pH 6.68.

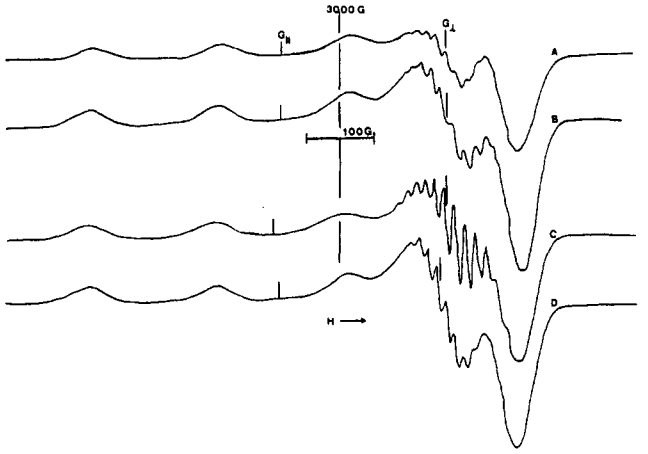

Figure 4. ESR spectra of mixed-ligand Cu^{II}(en)-like and Cu(en)L_n^{2+} species in Me_2SO/water glasses at 113 K: (A) [Cu(his)$_2$], 9.073 GHz, pH 10.00; (B) Cu(en)(imH)$_2^{2+}$, x = 3.0, 9.073 GHz, pH 6.60; (C) Cu(en)(imH)$_3^{2+}$, x = 10.0, 9.073 GHz, pH 6.62; (D) Cu(en)(py)$_2^{2+}$, x = 3.0, 9.072 GHz, pH 6.72.

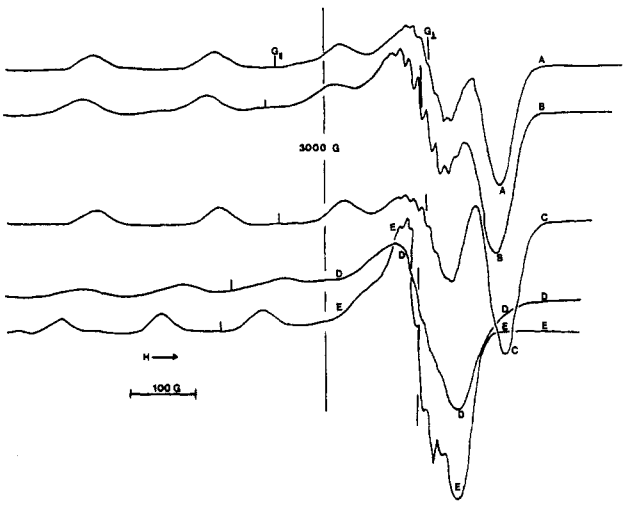

Figure 5. ESR spectra of mixed-ligand Cu^{II}(bpy)-like species in Me_2SO/water glasses at 113 K: (A) Cu(2-amp)$_2^{2+}$, 9.073 GHz, pH 10.45; (B) Cu(en)(py)$_2^{2+}$, x = 3.0, 9.072 GHz, pH 6.72; (C) Cu(en)(bpy)$^{2+}$, 9.073 GHz; (D) Cu(bpy)$_2^{2+}$, 9.073 GHz; (E) Cu(bpy)$(H_2O)_2^{2+}$, 9.072 GHz.

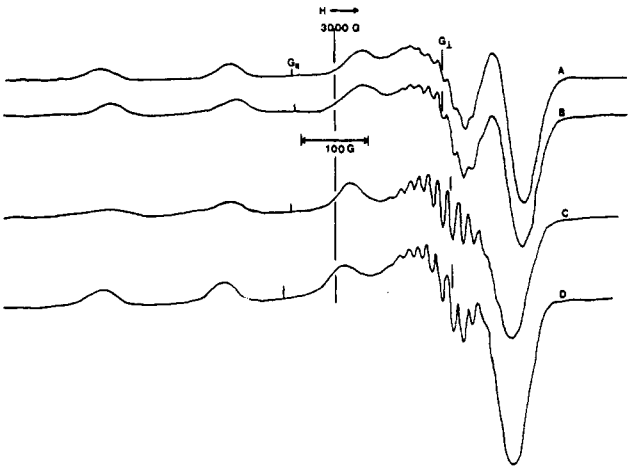

Figure 6. ESR spectra of mixed-ligand Cu^{II}(dien)-like species in Me_2SO/water glasses at 113 K: (A) Cu(dien)(imH)$^{2+}$, x = 3.0, 9.072 GHz, pH 5.85; (B) Cu(trien)(imH)$^{2+}$, x = 3.0, 9.072 GHz, pH 6.00; (C) Cu(trien)(imH)$_2^{2+}$, x = 20.0, 9.072 GHz, pH 6.30; (D) Cu(dien)(imH)$_2^{2+}$, x = 10.0, 9.072 GHz, pH 6.69.

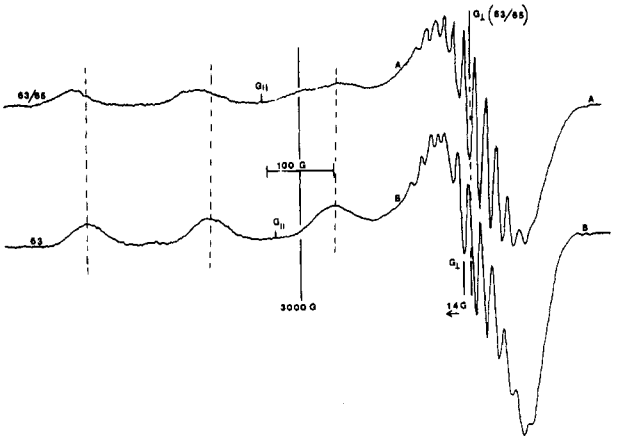

Figure 7. ESR spectra of ^{63}Cu-labeled complex (x = 5.0, 9.082 GHz, pH 6.87): (A) isotopic mixture; (B) $^{63}Cu(imCH_3)_5^{2+}$.

$(NO_3)_2$, $g_\parallel$ = 2.27 and 2.23, $g_\perp$ = 2.06 and 2.04, and $A_\parallel$ = 179 G.[14,15] [Cu(imH)$_4$]$(NO_3)_2$ was measured in a [Pd(imH)$_4$]$(NO_3)_2$

(14) Malmstrom, B. G.; Vanngard, T. *J. Mol. Biol.* **1960**, *2*, 118.

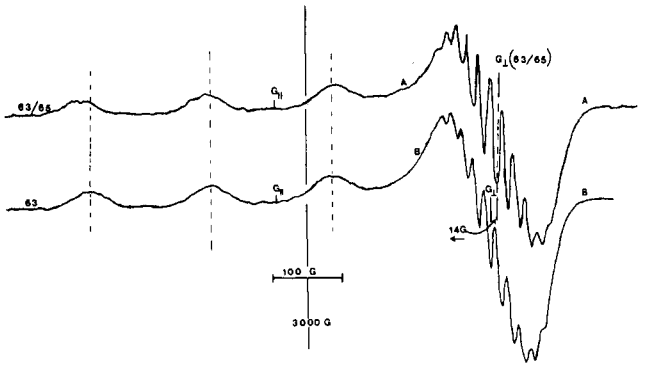

Figure 8. ESR spectra of ^{63}Cu-labeled complexes (x = 50.0, 9.083 GHz, pH 6.70): (A) isotopic mixture; (B) $^{63}Cu(imCH_3)_5^{2+}$.

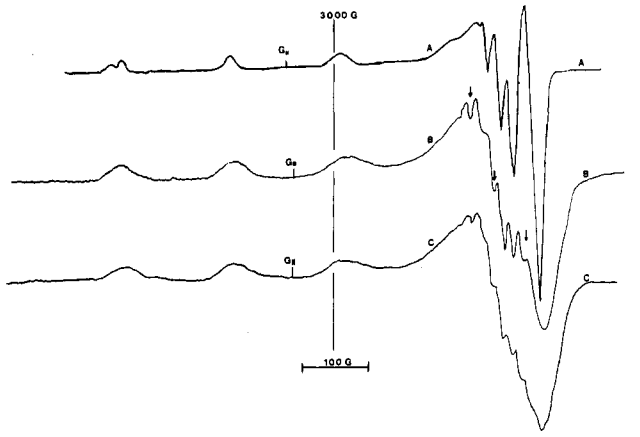

Figure 9. ESR spectra of $Cu(acac)_2$ complexes in 90:10 Me_2SO/H_2O glasses at 113 K: (A) $Cu(acac)_2$, 9.088 GHz, pH 7.10; (B) $Cu(acac)_2$(imH), x = 3.0, 9.088 GHz, pH 7.09; (C) $Cu(acac)_2(imH)_2$, x = 6.0, 9.088 GHz, pH 7.25.

host.[14] The differences displayed by $g_\parallel$, $g_\perp$, and $A_\parallel$ in the solid vs. the frozen glass illustrate the sensitivity of the method to minor changes in coordination geometry. Therefore, it is important to compare parameters between related complexes in the same medium, such as the Me_2SO/H_2O glass of our study.

$Cu(py)_4^{2+}$ (Figure 3sm) and $Cu(bpy)_2^{2+}$ (Figure 5D) show nearly identical $g_\parallel$, $g_\perp$, $A_\parallel$, and $A_\perp$(N) values; however, the degree of N-shf coupling implies that $Cu(bpy)_2^{2+}$ must be twisted away from square planar in order to reduce the N-shf structure compared to strong coupling in the $Cu(py)_4^{2+}$ case. At x = 1–10 the UV/vis spectra exhibit a continuous shift from 783 nm (n = 1) to 675 nm (n = 4) and 627 nm (n = 5). The dominant species at x = 4.0 and 5.0 are the CuL_4^{2+} and CuL_5^{2+} species, respectively, as implicated by ESR. The spectrum of $Cu(bpy)_2^{2+}$ has been examined in water/ethanol mixtures; cis and trans forms have been identified.[16] The values of $g_\parallel$ and $A_\parallel$ in the water/Me_2SO glass most closely match the parameters of the *trans*-diaqua complex of Marov et al.:[16] 2.27 and 164 in the Me_2SO/water glass and 2.28 and 165 ± 2 in the ethanol/water solution. Therefore, the structure appears distorted away from strictly trans toward the cis geometry by the twist, causing a reduction in N-shf structure.

The CuL_4^{2+} species (L = imH, $imCH_3$, py) are not severely split by rhombic distortion. The tendency of CuL_5^{2+} to undergo rhombic splitting may be measured by the separation between resonances which can be assigned as g_{xx} and g_{yy} portions of the $g_\perp$ region. The observed order is $Cu(imH)_5^{2+} \cong Cu(imCH_3)_5^{2+}$ (89 G) > $Cu(py)_5^{2+}$ (77 G) (Figure 1B, 2sm, and 4sm) following the relationship that imidazoles are stronger σ donors than pyridines, making it easier for the approach of two imidazoles and elongation of two other imidazoles to get the overall best in-plane bonds. It was previously reported that $[Cu(biimH)_2](ClO_4)_2$ exhibits N-shf lines with an axial type spectrum in the $g_\perp$ region in 90:10 CH_3NO_2/CH_3OH glass.[8] We confirmed this observation in this solvent (Figure 6sm). The axial spectrum suggests a nearly square planar complex with four N* contributions to the N-shf. It is apparent that the CH_3OH cosolvent is actually coordinated axially. When the same salt is dissolved in 9:1 CH_3NO_2/CH_3CN (Figure 5sm) or in 9:1 CH_3NO_2/CH_3OH (Figure 6sm) the spectra appear to be identical (axial). However, if the $[Cu(biimH)_2](ClO_4)_2$ salt is dissolved in either CH_3NO_2 alone or Me_2SO/water, the frozen-glass derivative spectra are less well-resolved (Figures 7sm and 8sm) with an additional feature on the high-field side of $g_\perp$, presumably from the presence of a second species.

^{63}Cu Isotopic Studies on $Cu(imCH_3)_5^{2+}$. A reviewer had disputed our assignment of the $Cu(imH)_4^{2+}$ and $Cu(imH)_5^{2+}$ spectra. His reasoning was based on the assumption that ^{63}Cu and ^{65}Cu isotopes would provide overlapped spectra such that two spectra contributing 9 N*-shf lines could overlap to display an 11-line net spectrum. This question was examined with use of the ^{63}Cu(II) isotope (see the Experimental Section) and the 1-methylimidazole complex in the range of x = 1.0–10.0. Above x = 5.0 the 11-line spectrum was again observed (cf. Figure 7). The pattern of the ^{63}Cu isotope (99.9% abundant) N-shf is the same as that of the isotopic mixture. The natural-abundance ^{63}Cu/^{65}Cu complexes provide the ESR derivative curve with N-shf shifted by about 14 G to higher field at the weighted average positions. But in all other regards the N-shf pattern is the same for the ^{63}Cu-labeled species. The comparison spectra for $^{63}Cu(imCH_3)_5^{2+}$ and $^{63,65}Cu(imCH_3)_5^{2+}$ at x = 50.0, where both UV/visible and ESR spectra are constant from x = 10.0 to x = 50.0, are shown in Figure 8.

Saturated N-Base Complexes. Both $Cu(en)(H_2O)_2^{2+}$ (Figure 2E) and $Cu(en)_2^{2+}$ (Figure 2D) exhibit strongly rhombically distorted spectra.[2] N-shf couplings are very weak at best, with weak shoulders corresponding to one active N donor per en (two for the $Cu(en)_2^{2+}$ species). Parameters for the saturated polyamine complexes are given in Table II. Good correspondence to data obtained in other laboratories is noted for both $Cu(en)(H_2O)_2^{2+}$ and $Cu(en)_2^{2+}$.[17] The rhombic splittings of g_{xx} and g_{yy} follow the order $Cu(en)(H_2O)_2^{2+}$ (70 G) < $Cu(en)_2^{2+}$ (90 G) < $Cu(trien)^{2+}$ (93 G) (Figures 3E and 2A,C, respectively). The degree of rhombic distortion is much greater for $Cu(en)_2^{2+}$ and $Cu(trien)^{2+}$ than for the analogous CuL_4^{2+} species of monodentate imH, $imCH_3$, or py donors. The presence of the chelate ring demands N–Cu–N angles that differ from 90°; in addition the stronger σ donors of the polyamines relative to the N* donors can further allow for rhombic in-plane effects. The case for $Cu(tren)(H_2O)^{2+}$ is different. This is a pseudo-trigonal-bipyramidal complex with one axial solvent donor.[9-11] The spectrum (Figure 3A) shows only four lines with $A_\perp$(Cu) of 123 × 10^{-4} cm^{-1} at $g_\perp$ = 2.20. No N-shf structure is detectable on any line; this complex is representative of the reversed EPR pattern. $Cu(tren)(H_2O)^{2+}$ forms a complex, adding one imidazole, *N*-methylimidazole, or pyridine (Figure 3B–D), showing 11 N-shf couplings on the $g_\perp$ fourth line of ca. 15.2 G. Values for $g_\perp$ and $A_\perp$(Cu) are 2.12 and 121 for imH, 2.16 and 121 for $imCH_3$, and 2.16 and 131 for py. Spectra of the $Cu(tren)L^{2+}$ adducts remain essentially unchanged in the ratio of [L]:[$Cu(tren)^{2+}$] from 3.0 to 50.0.

$Cu(en)L_n^{2+}$ Mixed-Ligand Complexes. Mixed-ligand complexes such as $Cu(en)(NH_3)_2^{2+}$ are well-known, but their ESR spectra lack N-shf structure of any intensity.[2,4] When imidazole is added to the $Cu(en)(H_2O)_2^{2+}$ complex, a new species is easily detected by the appearance of N-shf coupling in the low-field region of $g_\perp$ (g_{xx}). Spectra were obtained at x = $[imH]_i$:$[Cu(en)(H_2O)_2^{2+}]_i$ ratios of 3.0, 5.0, 6.0, 10.0, and 30.0. Nine N-shf lines are observed in the x = 5.0–10.0 concentration range. The spectra of the x = 3.0 (Figure 4B) and 5.0–10.0 species (Figure 4C) are not the

(15) (a) Massaresi, M.; Ponticelli, G.; Addepali, V. B.; Krishnan, V. G.; *J. Mol. Struct.* **1978**, *48*, 55. (b) Other imR complexes of the CuL_4^{2+} type have been reported: Massacesi, M.; Ponticelli, G.; Ramanchary, C.; Krishnan, V. G. *Transition Met. Chem. (Weinheim, Ger.)* **1980**, *5*, 353.

(16) Marov, I. N.; Belyaeva, V. K.; Smirnova, E. B.; Dolmanova, I. F. *Inorg. Chem.* **1978**, *17*, 1667.

(17) Lewis, W. B.; Alei, M.; Morgan, L. O. *J. Chem. Phys.* **1966**, *45*, 4003.

Table III. Mixed-Ligand Complexes of Cu(II) with Saturated Chain (N) and Aromatic (N*) Donors[a]

species	pH	$g_\parallel$	$g_\perp$	$10^4A_\parallel$, cm^{-1}	$A_\perp$(N), G	n
$Cu(en)(imH)_2^{2+}$	6.6	2.23	2.05	197	15	4
$Cu(en)(imH)_3^{2+}$	6.6	2.23	2.05	196	15	5
$Cu(en)(imCH_3)_3^{2+}$	6.6	2.24	2.04	195	15	5
$Cu(en)(py)_2^{2+}$	5.5–6.7	2.23	2.05	199	15	4
$Cu(en)(bpy)^{2+}$	...	2.21	2.05	196	14	3
$Cu(dien)(imH)^{2+}$	5.9	2.21	2.05	201	15	4
$Cu(dien)(imH)_2^{2+}$	6.7	2.22	2.04	192	15	5
$Cu(dien)(py)^{2+}$	6.8	2.21	2.05	205	15	4
$Cu(dien)(py)_2^{2+}$	7.0	2.21	2.05	204	15	5
$Cu(trien)(imH)^{2+}$	6.0	2.20	2.05	194	15	4
$Cu(trien)(imH)_2^{2+}$	6.7	2.21	2.04	181	15	5
$Cu(cyclam)(imH)^{2+}$	7.3–9.8	2.18	2.07	212	15	5
$Cu(his)_2^{2+}$	10.00	2.22	2.05	200	12 W	4
$Cu(amp)_2^{2+}$	10.45	2.22	2.05	193	13 VW	4

[a] pH varies by ca. 0.05 unit with x (defined in the text). Legend: his = histamine; amp = 2-(aminomethyl)pyridine.

same as those of $Cu(en)(H_2O)_2^{2+}$ or $Cu(imH)_4^{2+}$. At $x = 30.0$ en is replaced by two additional imH donors as the spectrum matches identically the spectrum of $Cu(imH)_5^{2+}$ in the Me_2SO/water glass; however, the UV/visible data suggest $Cu(en)(imH)_3^{2+}$ is present at room temperature. The spectra of the species in the range of $x = 3.0$–10.0 do not equal the sum of $Cu(en)(H_2O)_2^{2+}$ plus $Cu(imH)_4^{2+}$ spectra as clearly shown by a 45-G shift in the $g_\perp$ derivative minimum in the presence of imH ($x = 3.0$) relative to $Cu(en)(H_2O)_2^{2+}$. A reasonable match is achieved with the spectrum of $Cu(his)_2^{2+}$ (Figure 4A; his = histamine), which must have the $N_2N^*_2$ donor set. The same minimum is shifted 27 G less than for $Cu(en)_2^{2+}$. The mixed-ligand complexes $Cu(en)(imH)_2^{2+}$ and $Cu(en)(imH)_3^{2+}$ are implicated by these spectra. *The striking result is that incorporation of two or three N* donors activates the system in such a way that all N donors exhibit equivalent N-shf contributions.* At room temperature in 50:50 H_2O/Me_2SO the UV/visible spectra also show the coordination of imH. The maxima shift is as follows: $Cu(en)(H_2O)_2^{2+}$, 665 nm ($x = 0$); $Cu(en)(imH)(H_2O)^{2+}$, 597 nm ($x = 1.0$); $Cu(en)(imH)_2^{2+}$, 588 nm ($x = 3.0$). These results confirm the assignment of the dominant species as detected by ESR at these metal-to-ligand ratios. At $x = 30.0$ the UV/visible spectrum displays a maximum at 588 nm. This is not the same as the 606-nm value for $Cu(imH)_5^{2+}$ in the range of $x = 10.0$–50.0 (see above). Thus the five-coordinate adduct must be $Cu(en)(imH)_3^{2+}$ at room temperature, while the ESR-active species must be $Cu(imH)_5^{2+}$, which may be differentiated from $Cu(en)(imH)_3^{2+}$ on the basis of the extent of rhombic splitting of g_{xx} and g_{yy} lines (see below). The ESR parameters for mixed-ligand complexes are given in Table III. Virtually the same observations are obtained for L = $imCH_3$, which was studied at $x = [imCH_3]_i:[Cu(en)(H_2O)_2^{2+}]_i$ ratios of 3.0, 5.0, 6.0, and 10.0. The mixed-ligand species $Cu(en)(imCH_3)(H_2O)^{2+}$ and $Cu(en)(imCH_3)_3^{2+}$ are respectively implicated from 7 N-shf lines ($x = 3.0$; Figure 9sm) and 11 N-shf lines ($x = 5.0$–10.0; Figure 10sm) in the low-field $g_\perp$ region. The spectrum for $x = 3.0$ is ill-resolved and may represent a mixture of $Cu(en)L(H_2O)^{2+}$ and $Cu(en)L_2^{2+}$ species. For higher $imCH_3$:Cu(II) ratios (Figure 10sm) the mixed-ligand species show a 40-G shift to higher field in the $g_\perp$ minimum relative to the spectrum for $Cu(en)(H_2O)_2^{2+}$ and 27 G less shifted than the spectrum for $Cu(en)_2^{2+}$. Again, the presence of two or three N* bases activates all of the N donors in the mixed-ligand complex. Pyridine was studied with $Cu(en)(H_2O)_2^{2+}$ at ratios of 3.0, 5.0, 6.0, and 10.0. Only nine N-shf lines were detected for any species in this range, indicative of four nitrogen donors, e.g. $Cu(en)(py)_2^{2+}$ (Figure 5B). The spectrum of $Cu(en)(py)_2^{2+}$ is virtually the same as found with $Cu(amp)_2^{2+}$ (Figure 5A; amp = 2-(aminomethyl)pyridine). The $g_\perp$ minimum is shifted higher by 45 G relative to the signal for $Cu(en)(H_2O)_2^{2+}$ and 25 G less than the signal for $Cu(en)_2^{2+}$. The weaker σ donor, pyridine, is not sufficiently strong to add as an axial base, making a $Cu(en)(py)_3^{2+}$ species up through $x = 10.0$ while imH and $imCH_3$ form the analogous $Cu(en)L_3^{2+}$ species above $x = 5.0$. The extent of rhombic distortion appears to be similar in all of these complexes, $Cu(en)L_2^{2+}$ and $Cu(en)L_3^{2+}$, being 110 G for $imH(L_3)$, 100 G for $imCH_3(L_3)$, 111 G for $imH(L_2)$, and 114 G for $py(L_2)$ (average value 109 G). Note that the $Cu(en)L_3^{2+}$ species are more distorted than $Cu(imH)_5^{2+}$ by ca. 20 G greater separation in g_{xx} and g_{yy}. In addition the rhombic distortion for the $Cu(en)L_2^{2+}$ species exceeds that shown by only saturated amine donors such as $Cu(en)_2^{2+}$ or $Cu(trien)^{2+}$ by about 12 G.

The mixed complex $Cu(en)(bpy)^{2+}$ was prepared from 1:1:1 ratios of Cu^{2+}:en:bpy. The ESR spectrum (Figure 5C) showed the mixed-ligand complex shifted 40 G more than the signal for $Cu(en)(H_2O)_2^{2+}$ in the $g_\perp$ region. The N-shf structure is weaker than for $Cu(bpy)(H_2O)_2^{2+}$ (Figure 5E) but stronger than for $Cu(en)(H_2O)_2^{2+}$ (Figure 2E) or $Cu(bpy)_2^{2+}$ (Figure 5D). Only seven N-shf lines could be counted. The loss of four equally contributing N donors for this complex is taken to indicate some twist between the planes defined by $Cu(en)^{2+}$ and $Cu(bpy)^{2+}$ fragments. Indeed, the splitting of g_{xx} and g_{yy} components equals 121 G, larger than for any of the other mixed complexes and 7 G larger than for the related $Cu(en)(py)_2^{2+}$ case (Figure 5B).

$Cu(dien)L_n^{2+}$ and $Cu(trien)L_n^{2+}$ Mixed-Ligand Complexes. $Cu(dien)(H_2O)^{2+}$ was studied with imH and py as additional ligands. The x ratios were 3.0, 5.0, 6.0, and 10.0 for both imH and py. For $x = 3.0$ only a spectrum with nine N-shf, indicative of four N-shf active N donors, was observed in each case (Figures 6A and 11sm). The UV/visible spectra show a shift from 619 nm for $Cu(dien)(H_2O)^{2+}$ to 580 nm for the $Cu(dien)(imH)^{2+}$ complex and 600 nm for $Cu(dien)(py)^{2+}$. For $x \geq 5.0$ the spectra exhibit 11 N-shf features indicative of 5 N donors (Figures 6D and 12sm). The bis-adducts shift to 582 nm (imH) and 585 nm (py). ESR parameters are given in Table III. ^{63}Cu-labeled complexes also showed 11 N-shf lines at $x = 30$. Lippard et al. have reported for $Cu(tmdt)(imH)^{2+}$ the values[18] $g_\parallel = 2.21$ and $A_\parallel = 186$ at pH 6.2 compared to the values $g_\parallel = 2.21$, $g_\perp = 2.05$, and $A_\parallel = 201$ for $Cu(dien)(imH)^{2+}$ of this study at pH 5.9. The rhombic splitting parameters for the $Cu(dien)L^{2+}$ and $Cu(dien)L_2^{2+}$ complexes are for L 121 G (imH) and 118 G (py), and for L_2 99 G (imH) and 119 G (py). The rhombic splitting has increased slightly to an average of 114 G compared to 109 G for the $Cu(en)L_2^{2+}$ and $Cu(en)L_3^{2+}$ species. A curious observation was made in the study of $Cu(dien)L^{2+}$ and $Cu(dien)L_2^{2+}$ species (L = py, $imCH_3$). N-shf for $Cu(dien)(py)_2^{2+}$ was observed in frozen solutions that had been adjusted to pH $\geq$6.81 but was absent for a solution at pH 6.72 (Figures 12sm and 13sm). The two frozen solutions gave identical $g_\parallel$, $g_\perp$, $A_\parallel$, and rhombic splitting values. Only the N-shf was absent in the slightly more acidic sample. With $Cu(dien)(py)^{2+}$ nine N-shf features appeared in a frozen solution at pH 5.80 but were absent at pH 5.50. The N-shf coupling appears to have weaker intensity for the pyridine complexes with $Cu(dien)^{2+}$ than for the analogous imidazole species. Perhaps the pyridines and imidazoles undergo a proton-catalyzed exchange between coordinated and cage positions

(18) O'Young, C. L.; Dewan, J. C.; Lillenthal, H. R.; Lippard, S. J. *J. Am. Chem. Soc.* **1978**, 100, 7291.

that can lead to loss of N-shf even at 113 K. If this is the case, the axial and in-plane py ligands have slightly different barriers to exchange, with the axial exchange being more facile than the in-plane exchange. This is quite reasonable on ligand field grounds. The stronger imidazole donors exhibited a "pH window" in which N-shf spectra could be obtained only between pH 6.70 and 7.00. It would appear that ligand exchange requires interchange of the complexed ligand with the protonated form or a general acid must be present, but too high of a hydrogen ion donor accelerates the exchange to a time scale too fast for a "slow exchange" condition detectable by the presence of N-shf.

The spectra for Cu(trien) were obtained at x = $[imH]_i$:$[Cu(trien)^{2+}]_i$ ratios of 3.0, 10.0, and 20.0 (pH 6.00–6.70). The spectrum at x = 3.0 (Figure 6B) is identical with that of Cu(dien)$(imH)^{2+}$ (Figure 6A) while those at x = 10.0 and 20.0 (Figure 6C) match that of Cu(dien)$(imH)_2^{2+}$ (Figure 6D). Therefore, it is evident that the first imidazole adds at an in-plane location with rupture of one en-like ring of trien, but the next addition occurs at an axial coordination site without further displacement of the chelate structure. Five-coordinate complexes of Cu(trien)X^+, X^- = NCS^-, NO_3^-, etc., normally have the X^- anion added axially,[19] without disruption of the four in-plane Cu–N bonds. In the case of $Cu(en)^{2+}$ at x = 30.0 the en chelate ring is also disrupted; however, once the chelate ring of en is broken, the second amine is readily replaced by another imidazole to form $Cu(imH)_5^{2+}$. In the $Cu(trien)^{2+}$ case the existence of the dien-like fragment anchors the second amine of the ruptured first ring. Indeed, the spectrum at x = 10.0 and 20.0 does not match that of $Cu(en)(imH)_3^{2+}$, which would be the approximate site geometry if a greater portion of the trien rings were dislocated. It is worthwhile to point out that the addition of only one imidazole to an in-plane position, forming Cu(dien)$(imH)^{2+}$ or Cu(trien)$(imH)^{2+}$, is sufficient to induce N-shf structure of all in-plane N donors.

It may also be noted that only one imidazole or pyridine adds to Cu(tren)$(H_2O)^{2+}$ up through a [imH]:$[Cu(tren)^{2+}]$ ratio of 50.0. Unlike the case for the trien complex, the rupture of the first en-ring fragment will cause substantial strain at the apical N donor. Therefore, a 50-fold imH:Cu(II) condition is not sufficient to produce dissociation of the tren or a change from trigonal-bipyramidal coordination.

Cu(cyclam)$(imH)^{2+}$ Spectrum. It was of interest to discern if it is necessary to have at least one in-plane N* donor in order to achieve strong N-shf coupling of the other saturated amine donors of the various polyamines. The square-planar macrocyclic complex $Cu(cyclam)^{2+}$ (Figure 2B) was examined at x ratios of 1.0, 2.0, 4.0, and 10.0 with imH. All spectra were identical (Figure 2A) and showed 11 N-shf lines in a rhombically distorted ESR pattern. The data were collected in the pH range of 7.80–9.30 without discernible change in the N-shf intensities. From these results it is clear that axial addition of one imidazole donor which is rigorously restricted from in-plane coordination by the macrocyclic cyclam ligand is still sufficient to induce all 5 N-donor sites to become ESR-active, contributing to the 11 N-shf lines. The $g_\parallel$, $g_\perp$, and $A_\parallel$ values of Cu(cyclam)$(imH)^{2+}$ (2.18, 2.05, and 212) are similar to those of the $SC_6F_5^-$ axial adduct of $Cu(cyclam)^{2+}$ (2.20, 2.05, and 205).[20]

The ESR spectra of the red and blue isomers of Cu(tet a)$^{2+}$ and Cu(tet b)$^{2+}$ were also obtained (Figures 14sm–17sm) for correlation with low-frequency infrared studies of Cu(II) polyamines presented in a separate report.[29] All of these species have slight modifications of square-planar coordination at the Cu(II) site[21-23] except for Cu(tet b)$^{2+}$ (blue), which is trigonal bipyramidal.[23] The fifth site in Cu(tet b)$^{2+}$ (blue) is filled by solvent or X^- counterion. As anticipated, tet a (red and blue) and tet b (red) gave rhombically distorted ESR spectra with very weak N-shf couplings (Figures 14sm, 15sm, and 17sm) as indicated in Table II. The spectrum of Cu(tet b)$^{2+}$ (blue) (Figure 16sm) exhibited the reversed ESR pattern with $g_\perp$ = 2.14 and $A_\perp$(Cu) = 98 × 10^{-4} cm^{-1}. Therefore, the coordination of Cu(tren)$(H_2O)^{2+}$ with $g_\perp$ = 2.18 and $A_\perp$(Cu) = 123 × 10^{-4} cm^{-1} and the blue isomer of Cu(tet b)$^{2+}$ share similar features, while the other macrocycles are closer to $Cu(en)_2^{2+}$.

Cu(acac)$_2$(imH) Spectrum. A second test case of the ability to show N-shf coupling from a single axial N* donor was devised with use of square-planar $Cu(acac)_2$ in 90:10 Me_2SO/H_2O. The $Cu(acac)_2$ was too insoluble to give a sufficient concentration in the 50:50 glass. Spectra were obtained at $[imH]/[Cu(acac)_2]$ ratios of x = 0.0, 3.0, 6.0, and 60.0. The spectrum of $Cu(acac)_2$ reproduced the literature observations[24,25] ($g_\parallel$ = 2.27; $g_\perp$ = 2.03) including the 19-G I_{Cu} = $^3/_2$ coupling on the g_{xx} line, which is absent with H_2O or N and N* donors with Cu(II) (cf. Figure 9A). The frozen-glass ESR spectrum shows the presence of three additional lines when one axial imH donor is present (cf. Figure 9B) with x = 3.0 ($g_\parallel$ = 2.26, $A_\parallel$ = 176; $g_\perp$ = 2.06, $A_\perp$(N) = 45 G). At x = 6.0 substantial amounts of a disubstituted $Cu(acac)_2(imH)_2$ complex is detectable with the appearance of five N-shf lines ($g_\parallel$ = 2.26, $A_\parallel$ = 173; $g_\perp$ = 2.047, $A_\perp$(N) = 25 G). In this case, the six-coordinate species has redefined the stronger imH donors as "in-plane" ligands along with two oxygens of the acac donor. The axial ligands are forced to be the other mutually trans oxygen donors of the acac chelate (cf. Figure 9C). The $g_\parallel$ and $g_\perp$ values for $Cu(acac)_2(imH)_2$ are similar to the literature values for $Cu(acac)_2(en)$.[26] However, the $A_\parallel$(Cu) value is smaller for $Cu(acac)_2(imH)_2$ (173 vs. 202) but $A_\perp$(N) values are nearly the same (25 and 27 G). This suggests that the two imH donors are trans N* donors because $Cu(acac)_2(en)$ must have cis positions for its two N donors. Observation of five N-shf lines at x = 6.0 contrasts with the case of imH, itself, where six-coordination causes the loss of the N-shf interaction of the axial N* donors in competition with four other strong in-plane N* donors. The distortion that places the added imH donors as the strong-field axis donors is completely anticipated by the extent of rhombic distortion displayed by the CuL_5^{2+} species, L = imH or $imCH_3$ and py.

Conclusion. The ESR spectra of Cu(II) polyamines and mixed-ligand species prepared by the addition of imidazoles and pyridines have shown several features: (1) the complexes are increasingly rhombically distorted with increasing polyamine chain length; (2) the presence of even one aromatized (N*) donor will activate the N-shf coupling of all N donors in the first coordination sphere of Cu(II) in a tetragonal or rhombically distorted ligand field; (3) the additional N* donor may be either in-plane for CuN_4^{2+} donor sets or axial with CuN_5^{2+} donor sets to induce stronger N-shf coupling. The proper assignment of these species is evidenced by detection of four-, five-, and six-coordinate species whose ESR and UV/visible ligand field bands behave as required by square-planar, tetragonal, and distorted-octahedral complexes.

The desirable situation for saturated N donors remaining "silent" while imidazole donors are N-shf-active does not obtain in these systems. Therefore, the possibility to "count" the number of imidazole groups in copper(II) metalloproteins in the presence of saturated donors such as lysine residues is not realized. Furthermore, as distortions from simple tetragonal symmetry of a Cu(II) complex occur, there is a loss in intensity of N-shf coupling. With distorted geometries anticipated for most active sites of copper metalloproteins, there would appear to be even less chance to determine the number of imidazoles with accuracy. However, the presence of aromatized N donors at a copper(II) metalloprotein site may improve the chance of counting all N donors and thus be used to set a lower limit for its coordination number. Also, saturated N donors such as lysine have not been found previously

(19) Satry, B. A.; Osadullah, S.; Ponticelli, G.; Massacesi, M. *J. Chem. Phys.* **1979**, *70*, 2834.
(20) Addison, A. W.; Sinn, E. *Inorg. Chem.* **1983**, *22*, 1225.
(21) Clay, R.; Murray-Rust, J.; Murray-Rust, P. *J. Chem. Soc., Dalton Trans.* **1979**, 1135.
(22) Hay, R. W.; Clark, C. R. *J. Chem. Soc., Dalton Trans.* **1977**, 1148.
(23) Liang, B.-F.; Margerum, D. W.; Chung, C.-S. *Inorg. Chem.* **1979**, *18*, 2001.
(24) Goodman, B. A.; Raynor, J. B. *Adv. Inorg. Chem. Radiochem.* **1970**, *13*, 135.
(25) Maki, A. H.; McGarvey, B. R. *J. Chem. Phys.* **1958**, *29*, 31.
(26) Fritz, H. P.; Golla, B. M.; Keller, H. J. *Z. Naturforsch., B: Anorg. Chem., Org. Chem., Biochem., Biophys., Biol.* **1966**, *21B*, 97.

with Cu proteins. Therefore, presence of a countable N donor probably implicates presence of a histidine.

It has also been possible to get an ESR spectral match for species such as $Cu(en)(imH)_2^{2+}$ and $Cu(trien)(imH)^{2+}$ (having a pendant amine) by means of equivalent donor sets such as $Cu(his)_2^{2+}$ and $Cu(dien)(imH)^{2+}$. Therefore, the behaviors of various CuL_4^{2+} and CuL_5^{2+} donor sets are reasonably additive in terms of ESR parameters with simple monodentate plus simple chelate model assemblies. ^{63}Cu isotopic labeling has shown that both the ^{63}Cu and ^{65}Cu complexes exhibit equivalent N-shf couplings of 14 G.

The origin of the enhancement in the N-shf signal with the addition of an sp^2 N donor can be explained on the basis of the covalency of the bonding MO between Cu(II) and its σ donor ligands. The wave function for the bonding MO, ψ_b, can be written as a symmetry-adjusted linear combination (eq 1).[27] For a

$$\psi_b = a\, d_{x^2-y^2} + b\, d_{z^2} + C_1\, \sigma_{L_1} + C_2\, \sigma_{L_2} + \ldots + C_n\, \sigma_{L_n} \quad (1)$$

square-planar complex this is the B_{1g} MO with $b = 0$; $C_n = C_4$. The very weak coupling that is observed for $Cu(en)_2^{2+}$ or other all saturated N donors, combined with the observation of progressively stronger N-shf signals for $[CuN^*_4]^{2+} < [CuN^*_5]^{2+}$ species suggest that N-shf is observable only if the percentage of s character contributed by the nitrogen donors exceeds a critical value of 20.0% s. When all donors are sp^3, the detection level is borderline for N-shf coupling. However, if one or more ligands $L_1 \cdots L_n$ are of the sp^2 type, the percentage of N 2s character is increased in the resulting MO, ψ_b: 21% with one N* and three N donors up to 27% for four N* donors. In this manner the unpaired electron in a $d_{x^2-y^2}$ ground state (square planar or square pyramidal for Cu(II)) is brought into contact with all N centers to a greater degree by the addition of one or more ligands with a greater N 2s character. Since all are sp^2 donors for the $Cu(imR)_4^{2+}$ and $Cu(imR)_5^{2+}$ complexes, the percentage of N 2s component to ψ_b is maximized and the degree of N-shf is also maximized. This conceptual approach to explaining the effect of adding even just one N* donor to a complex which causes increased N-shf detectability has the additional attractive feature that all N donors will share approximately the same degree of contact with the unpaired electron via this MO as long as $|C_n|$ is nearly the same for each ligand. Therefore, all N donors will exhibit A_N of about the same value (14 G) unless the ligand's coefficient in ψ_b is very much less than any of the others due to structural changes. This latter point is rewarding in that for the $Cu(imCH_3)_6^{2+}$ species, formed at $x = 200$ $[imCH_3]:[Cu^{2+}]$ ratio, shows only strong N-shf for four of its in-plane donors; its coefficients for the axial donors C_5 and C_6 are very much smaller due to the Jahn-Teller distortion along the z axis.

There is a known theoretical basis for these results.[28] For frozen-solution spectra the measured value of A_N is the Fermi contact contribution (A_{FC}) to ligand superhyperfine coupling.[28] It is understood that A_{FC} is related to the s-orbital contribution α_s from which the % s character may be calculated (eq 2). As

$$A_{FC} = \frac{16\pi}{3}\gamma\beta\beta_N|\psi(0)|^2\alpha_s^2 \quad (2)$$

noted by Drago,[28] the existence and magnitude of A_N will be via the direct orbital coupling of the unpaired electron with the ligand through the MO in eq 1; spin polarization contributions are ignored. Indeed, the sp^3 donors are better candidates to exhibit stronger N-shf than the sp^2 ligands if spin polarization were important.

Acknowledgment. We express appreciation for support of this study under NSF Grant No. CHE 802183.

Supplementary Material Available: ESR spectra of Cu(II) complexes in Me_2SO/water glasses at 113 K (Figures 1sm-17sm) (7 pages). Ordering information is given on any current masthead page.

(27) Kivelson, D.; Nieman, R. *J. Chem. Phys.* **1961**, *35*, 149.

(28) Drago, R. S. *Physical Methods in Chemistry*; Saunders: Philadelphia, 1977; pp 488-487, and references therein.

(29) Diaz-Fleming, G.; Shepherd, R. E., submitted for publication in *Spectrochim. Acta, Part A*.

Contribution from the Corporate Research—Science Laboratories, Exxon Research and Engineering Company, Annandale, New Jersey 08801

Comparison of the Electronic Properties of $Mo_2O_2(\mu\text{-}S)_2(S_2)_2^{2-}$ and $Mo_2S_2(\mu\text{-}S)_2(S_2)_2^{2-}$

J. Bernholc*† and E. I. Stiefel*

Received April 22, 1985

A detailed theoretical analysis is presented of the similarities and differences of the electronic structures of $Mo_2O_2(\mu\text{-}S)_2(S_2)_2^{2-}$ (**1**) and $Mo_2S_2(\mu\text{-}S)_2(S_2)_2^{2-}$ (**2**). The analysis is based on self-consistent, first-principles electronic structure calculations for both systems. The replacement of the O atoms in **1** with S atoms in **2** leaves the higher filled MOs unaffected, although it removes the lower lying molecular orbitals corresponding to the Mo-O triple bond. The LUMOs, which in **1** are the Mo-O antibonding orbitals, are in **2** the Mo-S(terminal) antibonding orbitals at lower energies, decreasing the LUMO-HOMO gap in accordance with experimental observations. The energies of other antibonding orbitals are shifted somewhat to lower energies in going from **1** to **2**. The results suggest a similar reactivity pattern for reactions involving primarily the HOMO S_2 π^* orbitals, i.e., reactions with electrophiles. For reactions with nucleophilic components, somewhat lower activation energies should be expected due to the lowering of the HOMO-LUMO gap in **2** compared to that in **1**.

Introduction

The ions $Mo_2O_2(\mu\text{-}S)_2(S_2)_2^{2-}$ (**1**) and $Mo_2S_2(\mu\text{-}S)_2(S_2)_2^{2-}$ (**2**) belong to a large class of compounds that serve as models for active sites in molybdoenzymes[1] and in hydrodesulfurization and hydrodenitrogenation catalysts.[2] The isostructural ions consist of a formally $Mo_2O_xS_{4-x}^{2+}$ central core ($x = 2$ or 0) ligated by two S_2^{2-} diatomics (Figure 1).

$Mo_2O_2(\mu\text{-}S)_2(S_2)_2^{2-}$ was first synthesized in 1978 by thermal decomposition of $MoO_2S_2^{2-}$.[3] It reacts with activated acetylene in a highly unusual fashion by inserting the acetylene linkage into the terminal Mo-S linkage[4] to form a five-membered chelating

† Present address: Department of Physics, North Carolina State University, Box 8202, Raleigh, NC 27695.

(1) (a) Stiefel, E. I. In *Molybdenum and Molybdenum-Containing Enzymes*; Coughlan, M. P., Ed.; Pergamon: New York, 1980. (b) Spence, J. T. *Coord. Chem. Rev.* **1983**, *48*, 59. (c) Holm, R. H. *Chem. Soc. Rev.* **1981**, *10*, 454. (d) Averill, B. A. *Struct. Bonding (Berlin)* **1983**, *53*, 59. (e) Coucouvanis, D. *Acc. Chem. Res.* **1981**, *14*, 201.

(2) (a) Stiefel, E. I. Proceedings of the Climax Fourth International Conference on the Chemistry and Uses of Molybdenum; Barry, H. F., Mitchell, P. C. H., Ed.; Climax Molybdenum Co., Ann Arbor, MI, 1982. (b) Draganjac, M.; Simhon, E.; Chan, L. T.; Kanatzidis, M.; Baenziger, N. C.; Coucouvanis, D. *Inorg. Chem.* **1982**, *21*, 3322. (c) Miller, W. K.; Haltiwanger, R. C.; Van Derveer, M. C.; Rakowski DuBois, M. *Inorg. Chem.* **1983**, *22*, 2973 and references therein.

0020-1669/86/1325-3876$01.50/0